

Effect of neon plasma pre-irradiation on surface morphology and deuterium retention of tungsten

L. Cheng^a, G. De Temmerman^b, P. A. Zeijlmans van Emmichoven^b, G. Ji^c, H.B. Zhou^a, B. Wang^d, Y. Yuan^{a,*}, Y. Zhang^a, and G.H. Lu^{a,*}

^a *School of Physics & Nuclear Energy Engineering, Beihang University, Beijing 100191, China*

^b *FOM Institute DIFFER, Dutch Institute For Fundamental Energy Research, Association EURATOM-FOM, Trilateral Euregion Cluster, Nieuwegein, the Netherlands*

^c *Unité Matériaux et Transformations, UMR CNRS 8207, Université Lille 1, 59655 Villeneuve d'Ascq, France*

^d *College of Materials Science and Engineering, Beijing University of Technology, Beijing 100124, China*

Abstract

Neon and deuterium plasma irradiation of polycrystalline tungsten targets have been performed at high fluxes of $\sim 10^{24}$ ions $\text{m}^{-2}\text{s}^{-1}$ to study the interaction of neon with tungsten and the influence of neon on deuterium retention. Tungsten exposure to neon plasma leads to the formation of wavy nanostructures on the surface. Subsequent exposure to high-flux deuterium plasma leads to blister formation of micrometer size on top of the wavy structures. The total deuterium retention is decreased by neon pre-irradiation for all surface temperatures used in the present experiments. It is suggested that a barrier of trapped Ne is formed that interrupts the D transport and reduces D retention.

PACS: 52.40.Hf

PSI-21 Keywords: Deuterium inventory, Ion-surface interactions, Neon, Tungsten

** Corresponding Author Address:* School of Physics & Nuclear Energy Engineering, Beihang University, Beijing 100191, China

* *Corresponding Author email:* yueyuan@buaa.edu.cn (Y. Yuan) , LGH@buaa.edu.cn (G.H. Lu) :

Presenting Author: Long Cheng

Presenting Author e-mail: chenglong@phys.buaa.edu.cn

1. Introduction

Tungsten (W) is the material selected for the divertor target plates in ITER [1]. To avoid divertor damage by excessive heat flux the radiative power removal by means of impurity seeding (predominantly neon and nitrogen) is needed [2]. Understanding the interaction between seeded impurities such as neon (Ne) and tungsten, and their influence on the fuel retention and plasma-induced morphology changes is of particular interest. Experimental data exist for the interaction between another noble gas helium (He) and W and its influence on fuel retention. Strong reduction of deuterium (D) retention is observed for the cases of pre-exposure to He plasma as well as in the case of simultaneous D/He irradiation [3] [4] [5]. In the case of neon however, those data do not yet exist. The present paper describes the results from exposures of W targets to sequential Ne and D plasmas under ITER-like conditions in the linear plasma generator Pilot-PSI. The effect of Ne pre-irradiation on D retention at different surface temperatures and for a range of Ne fluences is investigated. Also the change of the W surface morphology induced by Ne-only, D-only and Ne-D sequential plasmas at different surface temperatures will be presented.

2. Experimental details

Polycrystalline tungsten targets (>99.95 wt.% purity) cut from a rolled sheet [6] were mechanically polished until the surface was mirror-like. An image depicting the typical surface after polish is shown in Fig. 1. Subsequently the targets were annealed at 1273 K for one hour at a background pressure of 5×10^{-4} Pa. The dimensions of the targets are 20 mm in diameter and 1.0 mm in thickness. The average grain size was 2-5 μm .

The W targets were exposed to neon (Ne) and deuterium (D) plasma in the linear plasma generator Pilot-PSI located at the FOM-Institute DIFFER. A detailed description of the machine can be found in [7]. The plasma is produced by a cascaded arc source and confined by an axial magnetic field of 0.4 T. Electron density and temperature of the plasma beam are measured by

Thomson scattering at a distance of ~ 20 mm from the surface. For exposure at surface temperatures of 400 K and 523 K, the plasma beam has a Gaussian profile with a peak electron density of about $3\text{-}4 \times 10^{20} \text{ m}^{-3}$ and a full width half maximum of ~ 1 cm. The peak electron temperature of the Ne and D plasmas are 2 and 1 eV respectively. The Ne and D ion fluxes are estimated from TS measurements, assuming that the ions are accelerated to sound speed at the sheath entrance (Bohm criterium), yielding 0.8 and $1.2 \times 10^{24} \text{ m}^{-2}\text{s}^{-1}$ respectively. For exposure at the surface temperature of 850 K the plasma was confined by a magnetic field of 0.8 T, yielding a flux of $(2\text{-}3) \times 10^{24} \text{ m}^{-2}\text{s}^{-1}$ for both Ne and D plasmas.

The incident ion energy is dominated by the target bias as the plasma potential is relatively small (a few V). For the Ne plasma, a bias of -20 V was used while it was set at -40 V for the D plasma case. The lower ion energy for the Ne case was chosen to avoid physical sputtering of the tungsten target and of the molybdenum clamping ring which is used to mount the tungsten target on the cooling unit. The temperature profile of the target surface is measured by an infrared camera (FLIR A645 sc) with an emissivity set to 0.05. The determination of the emissivity has been checked with other diagnostics (pyrometer and fast IR camera FLIR SC7500-MB). The shape of the temperature profile is similar to that of the electron density, a detailed description of the temperature profile can be found in [8]. The temperature difference between the center and the edge of the target was 80 K at 400 K and 523 K, and 200 K at 850 K. The reported surface temperatures as well as the ion fluxes and fluences are the ones at the center of the plasma beam, where the SEM observations were performed.

The targets were sequentially exposed to Ne plasma and to D plasma. Experiments were carried out for three surface temperatures of 400 K, 523 K and 850 K in the center of the plasma beam. For all three temperatures, two Ne fluences of $0.5 \times 10^{26} \text{ m}^{-2}$ and $1 \times 10^{26} \text{ m}^{-2}$ were used while the D fluence was kept constant at $1 \times 10^{26} \text{ m}^{-2}$ to be able to quantify the effect of Ne pre-exposure

on D trapping and retention. The $0.5 \times 10^{26} \text{ m}^{-2}$ and $1 \times 10^{26} \text{ m}^{-2}$ cases will be referred to as low and high Ne fluence in the following paragraphs.

The surface morphology of the tungsten targets was studied by a scanning electron microscope (SEM, Hitachi S-4700). The images were taken in the center of the plasma spot by using typically a 5 kV electron beam in secondary electron mode. Images of areas of 12 and 120 μm^2 were scanned to analyse the D blistering density on the surface.

The targets were analyzed by thermal desorption spectroscopy (TDS). The tungsten targets were heated up to 1273 K with a ramping rate of 1 K/s. The residual gases such as D_2 (mass 4), HD (mass 3), and Ne or D_2O (mass 20) were monitored by a quadrupole mass spectrometer (Balzers QMA 124). A calibration leak was used to determine the absolute sensitivity of the mass 2 and 4 signals. The sensitivity for mass 3 is assumed to be the average of the sensitivities for masses 2 and 4. When calculating the total D retention, D from HD and D_2 is taken into account.

3. Results

3.1. Surface morphology

Fig. 1 shows SEM images of the targets exposed to the different plasma species at different temperatures. In the Ne-only case, the W surface morphology is dominated by wavy nanostructures whose appearance depend on the grain orientation. While at 400 K the structure is only visible on a few grains, it is much more pronounced on the surfaces for exposure temperatures of 523 K and 850 K as shown in Fig. 1(b) and (c). The period of the wavy nanostructures is $9\text{-}26 \mu\text{m}^{-1}$, while the height was measured to be 2-10 nm by atomic force microscopy. The Ne fluence did not seem to have an influence on the surface morphology. In the D-only case, at 400 K, the surface is covered by a large number of small blisters having an irregular shape and a diameter of 0.1-0.5 μm as shown in Fig. 1(d). At 523 K, 0.1-0.5 μm sized blisters are still visible, but larger blisters with a diameter of 1-1.5 μm are also present as shown

in Fig. 1(e). A blister density calculation has been performed on the grains which show the most densely packed blisters, by calculating the total number of blisters divided by the corresponding grain area. At 400 K, the blister density is about $4 \mu\text{m}^{-2}$, and decreases to $2.8 \mu\text{m}^{-2}$ at 523 K. Targets exposed at 850 K exhibit no blister. The surface morphology of the targets sequentially exposed to Ne and D plasmas is characterized by a combination of the morphology changes induced by Ne- and D-only exposures. At 400 K and 523 K, blisters and wavy nanostructures co-exist on the surface, while at 850 K only the wavy nanostructure is observed. The blister density and size at 400 K and 523 K in the Ne-D sequential case are similar as they are in the D-only case, indicating the D blistering is not affected by Ne pre-irradiation.

3.2. Deuterium desorption

The D_2 desorption spectra for the targets exposed to D-only and Ne-D sequential plasmas are shown in Fig. 2 and grouped according to the exposure temperature. The targets exposed to D-only plasma at 400 K show a main desorption peak at 500 K and a small shoulder at higher temperature around 600-700 K. A deconvolution of the desorption spectrum was made using Gaussian curves revealing three desorption peaks at 500, 585 and 655 K with the 500 K peak being dominant. The intensity of the fitted 500 K peak is reduced by about 30% and 22% by Ne pre-irradiation with low and high fluence, respectively. The 585 K and 655 K peaks are also reduced in intensity and almost disappear in the Ne-D sequential case. The target exposed to D-only plasma at 523 K shows similar D desorption behavior compared to 400 K. Upon Ne plasma pre-irradiation, a decrease of the 500 K peak is observed whereas at 700 K a distinct peak is present. Applying the same fitting process as in the 400 K case, three desorption peaks at around 500, 600 and 700 K are found to reproduce the measurements. The integrated fitting results are shown in Table 1. In the fitting curves, besides the reduced 500 K peak intensity, the 700 K peak intensity increases from $6.7 \times 10^{16} \text{ m}^{-2}$ to $2.4 \times 10^{17} \text{ m}^{-2}$ and $1.7 \times 10^{17} \text{ m}^{-2}$ with the low and high Ne fluence pre-irradiation, respectively. The samples exposed at 850 K show a

different desorption behavior as compared to the previous cases. A peak at 620 K and a broad distribution at around 800-1000 K are observed in the D-only exposed target. Pre-irradiation with Ne leads to a strong suppression of the 620 K peak and to a reduction of the 800-1000 K distribution.

During the TDS experiments, the mass 20 signal was also recorded. We found that the desorption spectra of the mass 20 signal was very similar in all targets exposed to D-only and Ne-D sequential plasmas, suggesting that it predominantly consists of D₂O. The detection limit of Ne in the TDS experiments was estimated to be $\sim 10^{18} \text{ m}^{-2}$, from which we conclude that, at the time of the TDS (~ 1 week after plasma exposure), the total amount of Ne in W is lower than 10^{18} m^{-2} .

3.3. Total deuterium retention

The total D retention is plotted in Fig. 3 as function of the Ne fluence. The D retention varies with exposure temperature as well as with Ne pre-irradiation, i.e., the total retention is reduced in all targets exposed to Ne plasma. At 400 K, the reduction of the D retention does not vary a lot with the Ne fluence. 35 % and 32 % reduction is found in the low and high Ne fluence, respectively. In the targets exposed at 523 K and 850 K, the total retention is 2×10^{20} and $6.4 \times 10^{19} \text{ D m}^{-2}$ in D-only exposure, respectively. With the low and high Ne fluence pre-irradiation there is a reduction of 10 % and 30 % at 523 K and 68 % and 80 % at 850 K.

4. Discussion

Wavy nanostructures are observed on the targets exposed to Ne-only plasma at different surface temperatures. The dependence of the nanostructure formation on the grain orientation is consistent with Bradley Harper's model [9] based on Sigmund's sputtering theory [10]. As the Ne incident energy (20 eV) is lower than the sputtering threshold energy for W by Ne (40 eV [11]), the sputtering can be dominated by the high energy tail of the impacting Ne energy distribution. In Bradley Harper's model, the effect of thermally activated surface self-diffusion

is incorporated, which may explain the formation of nanostructures being more pronounced at 523 K and 860 K than at 400 K. The presence of a clamping ring made of molybdenum may affect the surface morphology by sputtering and deposition. Thus the target exposed to Ne plasma at 523 K was observed by X-ray photoelectron spectroscopy. The result shows no molybdenum peak, from which we conclude that the nanostructure is not affected by the deposition of molybdenum.

D retention is reduced by Ne pre-irradiation for all three exposure temperatures although the desorption behavior varies with temperature. For targets exposed at 400 K, the desorption peaks at 500 K and 600-700 K are reduced in the Ne-D sequential exposure. This may be caused by a diffusion barrier of trapped Ne being formed during Ne exposure. The effect is more pronounced at an exposure temperature of 850 K as a large reduction of the 620 K peak is observed in the Ne-D sequential exposure. Similar effects of He pre-irradiation have been reported in [4]. A reduction of the desorption peak was found in the He-D sequential exposure at 473-523 K in PISCES-A. A reduction of the D transport into the W bulk due to He pre-irradiation was proposed in [4].

Targets exposed at 523 K with Ne pre-irradiation show different D desorption behavior. Besides a reduced 500 K peak, an additional peak at 600-700 K is observed upon Ne pre-exposure. The 700 K peak corresponds to a trapping energy of 1.4-1.6 eV related to the plasma-induced modification, according to the measurement and simulation of D retention in W carried out in similar plasma and material conditions [12]. A trapping energy of 1.45 eV is related to atomic D trapped at a mono-vacancy or molecular D trapped at vacancy clusters [13]. Thus, an elevated 700 K peak indicates a plasma-induced damage such as vacancy formation. Though vacancy formation by collisional events is not expected for Ne at an incident energy of 20 eV, it could be triggered via clustering of trapped Ne. When a Ne cluster is large enough, it is able to spontaneously create Frenkel pairs. This effect has not yet been confirmed by other experiments

or by simulations as research on Ne-W interactions is rather scarce. However, for He, creation of vacancies and formation of clusters has been shown to occur in atomistic calculations [14] to explain observations of He trapping in perfect Ni [15]. In our experiments, the effect is most pronounced at 523 K, indicating an important role of temperature on the process.

5. Conclusion

In the present experiments, effects of Ne plasma pre-irradiation on surface morphology and D retention of W have been investigated. Ne plasma pre-irradiation leads to the formation of wavy nanostructures on the surface. Blisters of micrometer size on top of the wavy nanostructures were observed on targets subsequently exposed to D plasmas. TDS measurements show the D retention in W depends strongly on the exposure temperature, and the total D retention is decreased due to the Ne pre-irradiation under all investigated surface temperatures. It is suggested that during Ne exposure a barrier of trapped Ne is formed, thereby reducing the D transport to the bulk and the retention.

Acknowledgements

This work was supported by National Magnetic Confinement Fusion Science Program of China under Grant 2013GB109003 and the National Nature Science Foundation of China under contract No. 51401012. This work partially financially supported by the Nederlandse Organisatie voor Wetenschappelijk Onderzoek (NWO). The author would like to thank R.S. Al and M.J. van de Pol for the technical support in the Pilot-PSI experiment and M.H.J. 't Hoen for helpful discussions.

References

- [1] R. A. Pitts et al., 55th APS Meeting, Denver, CO, USA, paper WE1.00001
- [2] A. Kallenbach et al., Plasma Phys. Control. Fusion **55**, 124041 (2013)
- [3] D. Nishijima et al., Nucl. Fusion **45**, 669 (2005)

- [4] M. J. Baldwin et al., Nucl. Fusion **51**, 129501 (2011)
- [5] O. V. Ogorodnikova et al., J. Appl. Phys. **109**, 013309 (2011)
- [6] H. Y. Xu et al., J. Nucl. Mater. **443**, 452 (2013)
- [7] G. De Temmerman et al. Nucl. Fusion **51**, 073008 (2011)
- [8] M. H. J. 't Hoen et al., Nucl. Fusion **52**, 023008 (2012)
- [9] R. M. Bradley, J. Vac. Sci. Technol. A Vacuum, Surfaces, Film. **6**, 2390 (1988)
- [10] P. Sigmund, Phys. Rev. **184**, 383 (1969)
- [11] W. Eckstein, in *Sputtering by Part. Bombard.*, edited by R. Behrisch and W. Eckstein (Springer-Verlag, Berlin, 2007), pp. 33–187
- [12] M. H. J. 't Hoen et al., Nucl. Fusion **54**, 083014 (2014)
- [13] O. V. Ogorodnikova et al., J. Nucl. Mater. **390-391**, 651 (2009)
- [14] W. Wilson et al., Phys. Rev. B **24**, 5616 (1981)
- [15] G. J. Thomas et al., J. Appl. Phys. **52**, 6426 (1981)

Figure Captions

Fig. 1: Surface morphology of (a)(b)(c) W targets exposed to Ne plasma of $1 \times 10^{26} \text{ m}^{-2}$, (d)(e)(f) exposed to D plasma of $1 \times 10^{26} \text{ m}^{-2}$, (g)(h)(i) exposed to Ne-D sequential plasma. The exposure temperature is shown on the top of the figure. An image of polished surface without plasma exposure is shown in the lower left.

Fig. 2: TDS D_2 desorption profiles for W targets exposed to D-only, Ne-D sequential plasmas at 400 K, 523 K and 850 K. The heating rate was 1 K/s for all samples. The vertical axis scale of (c) is smaller than that of (a) and (b).

Fig. 3: Total amount of D retained in W targets exposed to D-only, Ne-D sequential plasmas at exposure temperature of 400 K, 523 K and 850 K as determined by TDS.

Figure 1.

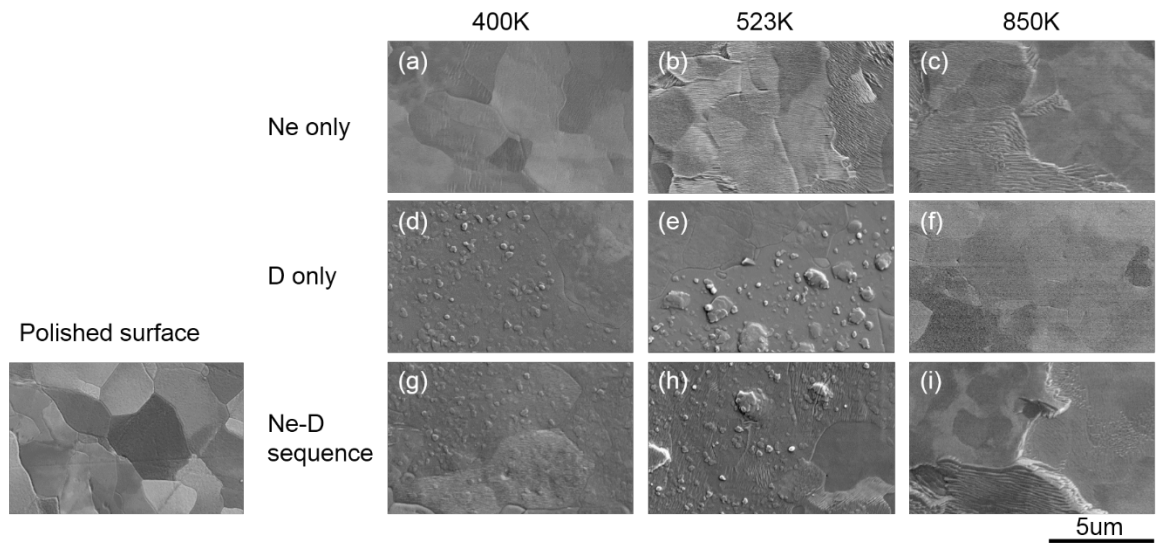


Figure 2.

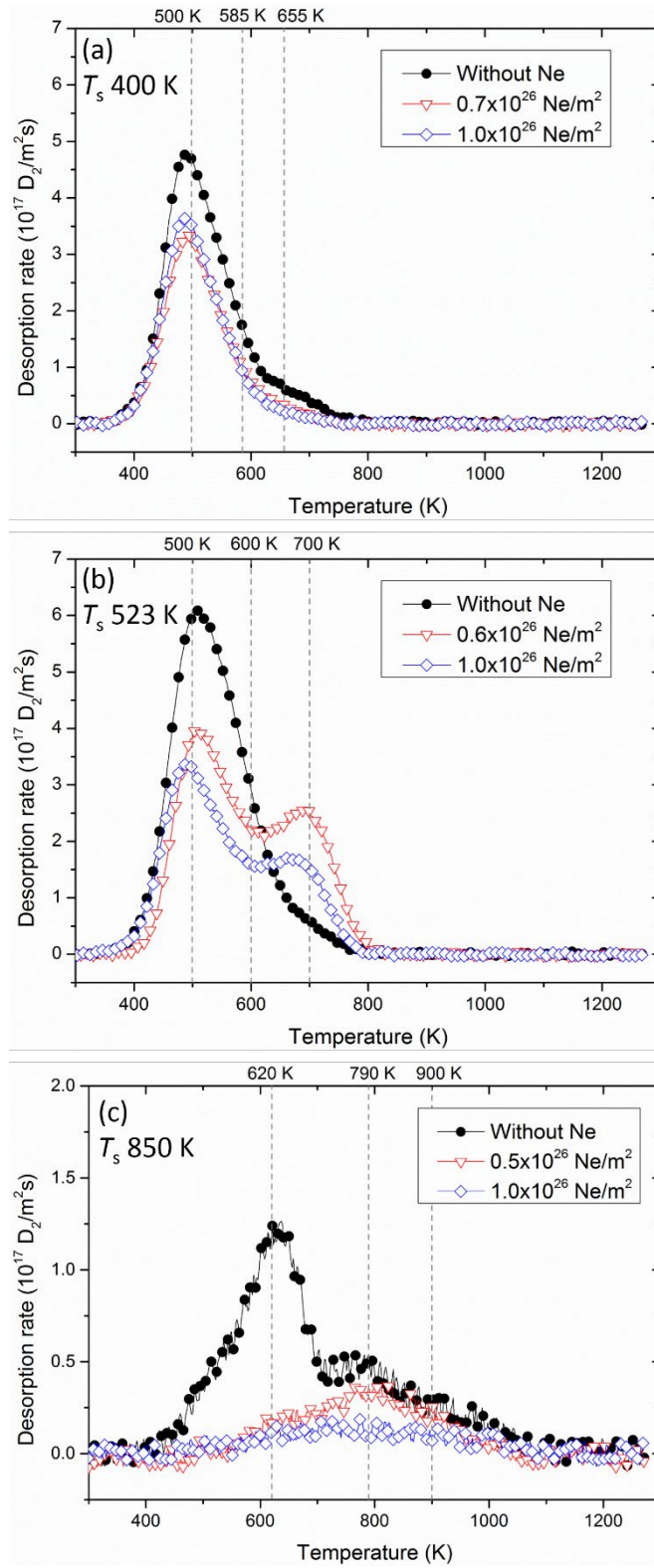
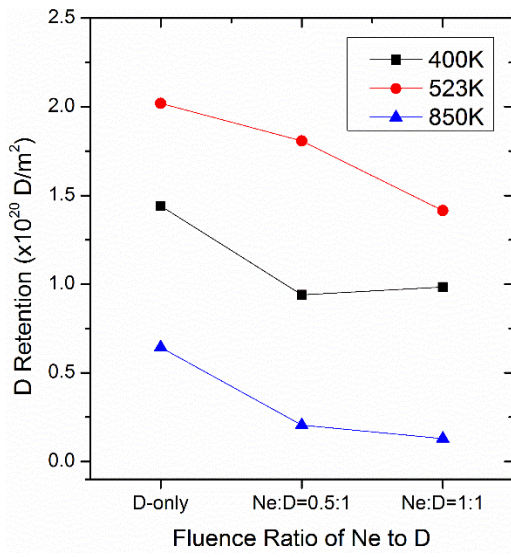


Figure 3



	Peak intensity at 490-510 K (m ² s ⁻¹)	Peak intensity at 581-594 K (m ² s ⁻¹)	Peak intensity at 680-700 K (m ² s ⁻¹)
Without Ne	6.0 × 10 ¹⁷	1.8 × 10 ¹⁷	6.7 × 10 ¹⁶
0.6 × 10 ²⁶ /m ²	3.6 × 10 ¹⁷	1.9 × 10 ¹⁷	2.4 × 10 ¹⁷
1.0 × 10 ²⁶ /m ²	3.3 × 10 ¹⁷	1.3 × 10 ¹⁷	1.7 × 10 ¹⁷

Table 1. Fitting parameters of TDS for targets at exposure temperature of 523 K.